

Evidence for a charge Kondo effect in $\text{Pb}_{1-x}\text{Tl}_x\text{Te}$ from measurements of thermoelectric power

M. Matusiak,^{1,2} E. M. Tunncliffe,¹ J. R. Cooper,¹ Y. Matsushita,^{3,4} and I. R. Fisher^{3,5}

¹*Cavendish Laboratory, Department of Physics, University of Cambridge, J.J. Thomson Avenue, Cambridge CB3 0HE, United Kingdom*

²*Institute of Low Temperature and Structure Research, Polish Academy of Sciences, P.O. Box 1410, 50-950 Wrocław, Poland*

³*Department of Applied Physics and Geballe Laboratory for Advanced Materials, Stanford University, Stanford, California 94305-4035, USA*

⁴*Department of Materials Science and Engineering and Geballe Laboratory for Advanced Materials, Stanford University, Stanford, California 94305-4035, USA*

⁵*Stanford Institute for Materials and Energy Science, SLAC National Accelerator Center, 2575 Sand Hill Road, Menlo Park, California 94025, USA*

(Received 15 October 2009; published 9 December 2009)

We report measurements of the thermoelectric power (TEP) for a series of $\text{Pb}_{1-x}\text{Tl}_x\text{Te}$ crystals with $x=0.0$ to 1.3%. Although the TEP is very large for $x=0.0$, using a single-band analysis based on older work for dilute magnetic alloys we do find evidence for a Kondo contribution of 11–18 $\mu\text{V}/\text{K}$. This analysis suggests that T_K is $\approx 50\text{--}70$ K, a factor 10 higher than previously thought.

DOI: [10.1103/PhysRevB.80.220403](https://doi.org/10.1103/PhysRevB.80.220403)

PACS number(s): 72.15.Qm, 72.15.Jf, 74.70.Ad

The traditional “spin” Kondo effect occurs in a nonmagnetic host metal containing a small concentration of magnetic impurities. Here the antiferromagnetic exchange interaction (J) between the local magnetic moment and the conduction electrons gives rise to a $-|J|^3 \log T$ term in the temperature (T) dependent electrical resistivity $\rho(T)$ and other unusual properties^{1–3} including an anomalously large and T -dependent thermoelectric power (TEP or S). Below the Kondo temperature (T_K) which can be extremely small, the spin of the impurity is compensated by a cloud of conduction-electron spins extending over distance $\sim \hbar v_F / k_B T_K$, where v_F is the Fermi velocity of the host metal. There is a “triple peak” in the impurity density of states (DOS),³ with two side lobes derived from the spin-split virtual bound state and a narrow peak of width $k_B T_K$ at the Fermi energy. It is thought⁴ that a similar description applies to the charge Kondo effect discussed here.

Experimental⁵ and theoretical⁴ evidence has been reported for a charge Kondo effect in $\text{Pb}_{1-x}\text{Tl}_x\text{Te}$ crystals with $x \geq 0.3\%$. It arises because Tl^+ and Tl^{3+} ions both have filled shells, i.e., $6s^2$ and $6s^0$, that can be more stable than the $6s^1$ state of Tl^{2+} . So when Tl is in an environment favorable for divalency there can be two degenerate, or nearly degenerate, nonmagnetic charge states Tl^+ and Tl^{3+} that can be described by the Anderson model and can also give rise to a Kondo effect.⁴ The resulting charge fluctuations are thought to be important for superconductivity^{4–6} in $\text{Pb}_{1-x}\text{Tl}_x\text{Te}$. In the present Rapid Communication we report TEP data for single crystals of $\text{Pb}_{1-x}\text{Tl}_x\text{Te}$ and discuss evidence for an anomalous contribution associated with a charge Kondo effect.

The crystals of $\text{Pb}_{1-x}\text{Tl}_x\text{Te}$ with $x=0, 0.2, 0.3, 0.6, 1.1,$ and 1.3% were from the same preparation batches studied previously.^{5–7} Their thermopower was measured using CuBe wires,⁸ whose TEP was measured separately relative to a cuprate superconductor and found to be small with a maximum of 0.2 $\mu\text{V}/\text{K}$ near 30 K. Initially the temperature gradient, ΔT , was measured using a constantan-chromel thermocouple made of 25 μm diameter wires, and glued to the mm-sized crystals with GE varnish, but for the data reported here very small diode thermometers⁸ were used. These were

less straightforward to mount, but gave more reliable measurements of ΔT , especially at low T where the sensitivity of the thermocouple decreases. The diodes were also attached to the sample using GE varnish, and the distance between them, measured to ± 3 to 5% using a binocular microscope, is the main source of error in the TEP.

For many dilute metallic alloys $\rho(T)$ approximately obeys Matthiessen’s rule which states that the contributions ρ_j arising from two or more different scattering mechanisms ($j=0, 1, 2, \dots$) are simply additive. It generally holds reasonably well when T is comparable to the Debye temperature (Θ_D) or when the impurity resistivity is smaller than that caused by electron-phonon scattering, but at lower T there can be significant deviations. One probable reason is that conservation of crystal momentum (\mathbf{k}) is less strict in an alloy because the finite electron mean-free path limits the size of electron wave packets.⁹ The equivalent Nordheim-Gorter (NG) rule¹⁰ for combining contributions S_j^d to the total electron diffusion TEP S^d from different scattering mechanisms in the same band is

$$S^d = \frac{\sum_j S_j^d \rho_j}{\sum_j \rho_j}. \quad (1)$$

It relies on Matthiessen’s rule being obeyed and on the scattering being effectively elastic, which is only true for $T \geq \Theta_D$ or in the residual resistivity (ρ_{res}) region. Resistivity data⁷ for $\text{Pb}_{1-x}\text{Tl}_x\text{Te}$ crystals from the same preparation batches are shown in Fig. 1. Matthiessen’s rule is obeyed reasonably well for $x \geq 0.6\%$ for all T and for $x=0.3\%$ for $T < 150$ K. The insert shows that ρ_{res} is small for $x \leq 0.2\%$ but then increases linearly with x for $x \geq 0.3\%$. This is consistent with other evidence that valency skipping sets in near $x=0.3\%$ (Ref. 5) and, together with Matthiessen’s rule, implies that there are no gross changes in electronic structure at higher x . The linearity also suggests that the Tl impurities act as independent scattering centers for $x \geq 0.3\%$. TEP data measured for the six samples are shown in Fig. 2. All Tl-doped samples have $S \sim 100\text{--}140$ $\mu\text{V}/\text{K}$ at 300 K with

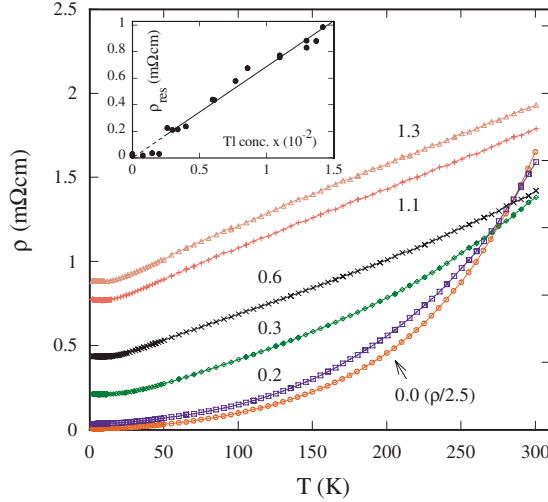


FIG. 1. (Color online) resistivity vs temperature for $\text{Pb}_{1-x}\text{Tl}_x\text{Te}$ crystals (Ref. 7) from the same preparation batches as those studied here, values of x given in %. The inset shows residual resistivity vs x for all crystals measured, $\rho(T)$ data for all x values in the insert are given in Ref. 7.

similar slopes and a positive curvature at lower T , while the pure PbTe sample has a larger TEP, $300 \mu\text{V}/\text{K}$ at 300 K , and a negative curvature.

Analysis of various Kondo alloys (e.g., AuFe , AuMn , and AuCr) (Refs. 11 and 12) suggests that S^d in Eq. (1) contains three terms, S_0 , S_1 and S_K . S_0 arises from the energy dependence of the potential scattering term V in the Kondo Hamiltonian, and is related to the energies and widths of the $3d$ virtual bound states. It is linear in T and in Eq. (1) is weighted by $\rho_{\text{res}} \equiv \rho_0$. The electron-phonon scattering term, S_1 , is also expected to be linear in T both for $T \geq \Theta_D/5$ and $T < \Theta_D/10$ but with a factor of 3 smaller slope at low T . For PbTe, heat-capacity data⁶ give $\Theta_D = 168 \text{ K}$. S_0 , S_1 , ρ_0 , and ρ_1 are often calculated using first-order perturbation theory, while S_K , the Kondo TEP contribution, arises from higher order scattering processes involving noncanceling Fermi factors. It is also weighted by ρ_0 in Eq. (1). A broad peak in S^d is often observed near the Kondo temperature T_K , and often used to estimate T_K .^{3,13} However it has been argued that S_K could be constant for $T \geq T_K$,^{11,14} as predicted by high T perturbation theory² and that the fall above the peak is caused by the other T -dependent terms in Eq. (1). For $T \leq 0.1-0.15T_K$,¹⁴ S_K falls to zero as T^1 , and fits $S_K = AT/(T+0.35T_K)$ for $T \leq T_K$.

In view of the above discussion, we expect S_K to be constant or to fall slowly with T above a cutoff temperature $T_0 > T_K$, and so above T_0 Eq. (1) gives

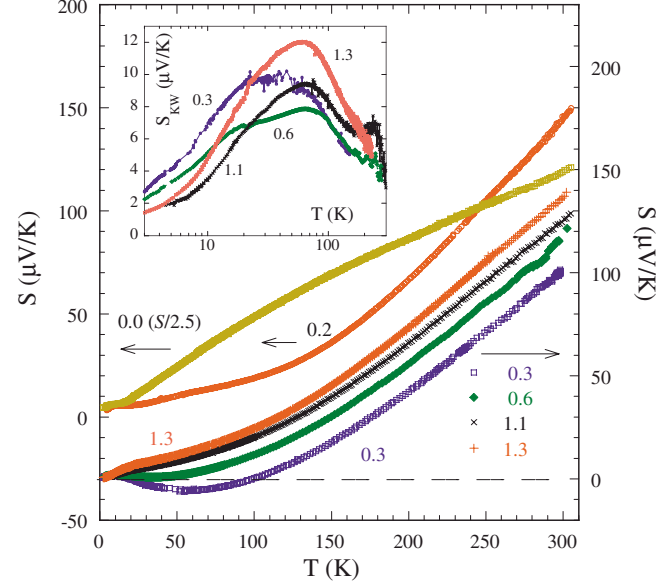


FIG. 2. (Color online) measured values of the TEP for $\text{Pb}_{1-x}\text{Tl}_x\text{Te}$ crystals with $x=0.0$ and 0.2% left-hand scale and $x=0.3, 0.6, 1.1,$ and 1.3% right-hand scale. The inset shows the weighted Kondo contribution, $S_{KW} \equiv S_K \rho_0 / \rho(T)$ for the values of $x(\%)$ shown.

$$S = \frac{\alpha T \rho_0 + \beta T \rho_1 + \gamma \rho_0}{\rho_0 + \rho_1(T)} \quad (2)$$

where α , β , and γ are independent of x and T . Fits to Eq. (2) were made from 300 K to $T_0 = 90, 70, 50,$ or 30 K , with α , β and γ as free parameters and ρ_0 and $\rho_1(T)$ obtained by fitting the data in Fig. 1 to $\rho = A + BT + CT^2$. Values of α , β , and γ and A , B , and C are given in Table I. $T_0 = 70 \text{ K}$ gave slightly better fits. Fits from 150 to 70 K gave similar results and for $x=0.3\%$ we used this range because of the curvature in $\rho(T)$ shown in Fig. 1 for this sample. Below 70 K , $S_K(T)$ was obtained from Eq. (2) by using the formula $S_K(T) = S_{\text{meas}} \rho / \rho_0 - \alpha T - \beta T \rho_1 / \rho_0$ and is shown in the main part of Fig. 3(a). Our fitting procedure should give a constant value for S_K above 70 K . The variations seen in Fig. 3(a) arise from residual errors in the fits multiplied up by ρ / ρ_0 and are only a few times the noise level.

For an isotropic parabolic band with Fermi energy E_F , $\beta \approx \pi^2 k_B^2 / (eE_F)$ for $T \geq \Theta_D/5$ and $\pi^2 k_B^2 / (eE_F)$ for $T \leq \Theta_D/10$,^{10,16} i.e., $T \leq 17 \text{ K}$ for PbTe. The β values in Table I give E_F between 73 to 160 meV so their sign and magnitude are reasonably consistent with E_F being measured relative to the bottom of the Σ band,⁷ despite the fact that the

TABLE I. Fitting parameters, A , B , and C , for $\rho(T)$ and α , β , and γ , for TEP.

$x\%$	A mΩ cm	B mΩ cm/K	C mΩ cm/K ²	α μV/K ²	β μV/K ²	γ μV/K
0.3	0.2017	1.080×10^{-3}	9.29×10^{-6}	-0.581	0.446	14.3
0.6	0.4124	2.315×10^{-3}	3.37×10^{-6}	-0.362	0.682	11.5
1.1	0.7371	3.343×10^{-3}	5.97×10^{-7}	-0.211	0.837	12.1
1.3	0.8472	3.640×10^{-3}	-2.6×10^{-8}	-0.211	0.947	17.7

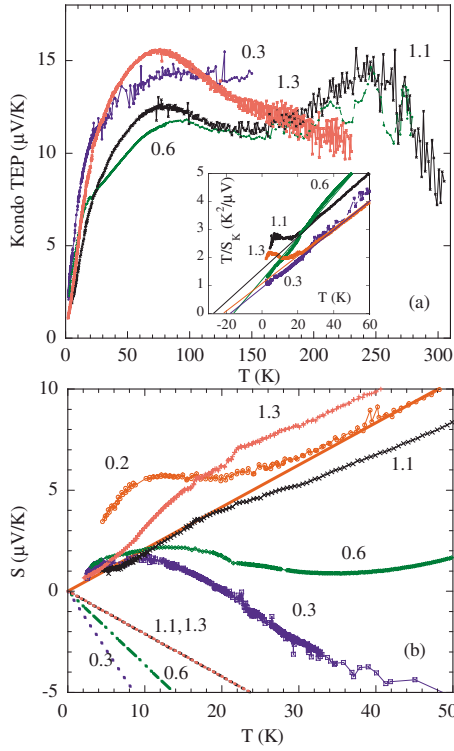


FIG. 3. (Color online) (a) Kondo contribution to the TEP of Pb_{1-x}Te single crystals with values of x shown in %. The insert shows T/S_K vs T plots used to find T_K from the empirical, low T , law (Ref. 14, $S_K = AT/(T + 0.35T_K)$). (b) Raw TEP data for the values of x in % shown. A solid line shows S^d for $x=0.2\%$ and dashed lines show αT for $x \geq 0.3\%$

hole pockets are actually ellipsoidal. But the changes of β with x are not understood since Hall data⁶ suggest a slight increase in hole concentration, i.e., in E_F with x . The magnitudes of α are similar to β but of opposite sign corresponding to higher energy holes being more strongly scattered by the TI impurities. Within a Kondo picture this arises from the asymmetry of the Friedel-Anderson virtual bound states describing the valency fluctuations, but a low value of E_F for the Σ band could also affect α . Finally the values of γ ranging from 11 to 18 $\mu\text{V}/\text{K}$ are similar to those associated with the traditional Kondo effect and the asymmetric Anderson model.

Fits to Eq. (2) for the $x=0.0$ and 0.2% samples were not good and are not shown. As shown in Fig. 1 for these two samples ρ_{res} values are very low and $\rho(T)$ much more curved than for $x \geq 0.3\%$. These differences and Hall data⁶ suggest that the L band dominates electronic transport for low x while for $x \geq 0.3\%$ the Σ band plays a leading role.^{5,7} The TEP of the 0.2% crystal varies as AT between 40 and 100 K with $A=0.2 \mu\text{V}/\text{K}^2$ but rises sharply at higher T . This value of A is reasonably compatible with $E_F=200$ meV obtained from analysis of Hall data⁶ but the strong increase at higher T is not understood. The deviations from linearity for $x=0.2\%$ shown in Fig. 3(b) are ascribed to the gradual onset of phonon drag below 40 K. This is considerably lower than for most metals where it is usually $\approx \Theta_D$ (Ref. 10) and may arise because both the L and Σ hole pockets have small Fermi wave vectors (k_F). So electron-phonon scattering

within a pocket will be suppressed to lower T until typical phonon wave vectors $\sim (T/\Theta_D)(\pi/a)$, where a is the lattice spacing, become smaller than $2k_F$. We cannot assume that phonon drag corrections for the Σ band, i.e., $x \geq 0.3\%$, will be similar to those for $x=0.2\%$. Perhaps the only way to obtain the phonon drag term for $x \geq 0.3\%$ is to suppress superconductivity by applying a magnetic field and measure to much lower T where it will eventually vary as T^3 . Below $T \sim 8$ K the raw data in Fig. 3(b) show an approximately T -linear, and x -independent decrease that is typical of the Kondo effect for $T \lesssim 0.1-0.2 T_K$.¹⁴ However according to the preceding analysis the αT terms shown by the dashed lines in Fig. 3(b) are still present at low T . They should be subtracted to obtain $S_K(T)$ and this spoils the x independence to some extent.

We estimated T_K using two methods. The first one is based on the widely held view^{3,13} that there is an x -independent peak in the TEP at T_K in dilute magnetic alloys, where the host metal has a very small TEP. If the TEP of the PbTe host metal and S_0 were both small then we would measure a weighted value $S_{KW} \equiv S_K \rho_0 / \rho$. Plots of S_{KW} found in this way, using the $S_K(T)$ data in Fig. 3 are shown in the insert to Fig. 2. We see that there are indeed broad peaks near 60 K for $x=0.6, 1.1,$ and 1.3% . The second method is based on the empirical law $S_K = AT/(T + 0.35T_K)$ (Ref. 14) for which plots of T/S_K vs T give a straight line extrapolating to $S_K=0$ at $-0.35T_K$. As shown in the insert to Fig. 3(a) such plots are reasonably linear and give T_K values ranging from 45 to 75 K for the four samples. The deviations below 20 K for $x=1.1$ and 1.3% could arise from phonon drag. Values of T_K obtained in these two ways are significantly higher than $T_K \sim 6$ K,⁵ which was estimated by fitting resistivity data to $\rho = \rho(0)[1 - (T/T_K)^2]$ but with considerable uncertainty in the appropriate value of $\rho(0)$. On the other hand, using the fact that the T^2 law normally extends up to $0.1 T_K$ (Ref. 15) gives $T_K \geq 40$ K in closer agreement with our estimates from the TEP.

Although we should be cautious about applying spin Kondo formulas to a doped semiconductor, PbTe, the observation of Matthiessen's rule is consistent with a single-band metallic picture and minor changes in hole concentration above $x=0.3\%$. Taking $T_K=60$ K (Ref. 17) does affect some of the previous conclusions.^{5,6} For example on the basis of the measured specific-heat coefficient $\gamma(0)$ and the depth of the resistivity minimum it was suggested^{5,6} that only $x_{eff}/x \sim 0.01$ of the TI impurities were degenerate to within $T_K=6$ K and hence only these were effective Kondo scatterers. With $T_K=60$ K, x_{eff}/x becomes ~ 0.1 and also the radius of the charge cloud is smaller, ~ 25 nm, taking $k_F=10^7 \text{ cm}^{-1}$ and $m=0.6m_e$, i.e., $v_F=2 \cdot 10^7 \text{ cm/s}$. Accordingly at $x=1\%$, on average there would still be about 10 other TI atoms within the charge cloud of one impurity, but because $x_{eff}/x \sim 0.1$ only one of these would be a Kondo scatterer. We note that the charge clouds must overlap and be delocalized at low T (as are the Kondo states in heavy Fermion superconductors) because otherwise they would not contribute to superconductivity and there would be a residual $\gamma(0)$ in the superconducting state. Such considerations of charge overlap may make detailed analysis in terms of the L and Σ bands of undoped PbTe less straightforward than previously thought.

Assuming that there is also a narrow peak $\sim k_B T_K$ wide in the DOS for charge Kondo impurities, then the field scale for magnetotransport effects is larger $\sim k_B T_K / \mu_B$. Also one would expect a magnetic-susceptibility contribution $\chi(T) = \mu_B^2 x_{eff}^2 N_{AV} / k_B (T + T_K)$ emu/mole where N_{AV} is Avogadro's number, μ_B , the Bohr magneton. For $x_{eff} \sim 0.1x$, this would be undetectable in the available $\chi(T)$ data^{5,7} but might show up in detailed measurements and analysis, like those made for AlMn alloys.¹⁸ There are some indications that x_{eff}/x could be larger than 0.1. Using the formula³ $\gamma(0) = 0.4128 \pi^2 k_B / (6T_K)$ gives $\gamma(0) = 0.94$ mJ/mole/K² for $x = 1\%$ compared with the average slope from the *raw* experimental data⁶ of $\gamma(0)/x = 0.57$ mJ/mole/K²/%, implying that $x_{eff}/x \approx 0.6$. We also note that the measured values of $\Delta\chi(0)/\Delta\gamma(0)$ are remarkably close to $6\mu_B^2/\pi^2 k_B^2$, the value expected from spin Kondo theory, namely a Wilson ratio of 2 rather than 1 for noninteracting fermions. However for $x_{eff}/x \approx 0.6$ it is difficult to understand the T dependence

since the $\chi(T)$ curves for x between 0.3 and 1.3% are essentially parallel. Although the effective mass and band gap of PbTe are T dependent,¹⁹ it seems unlikely that this would exactly compensate any $1/(T+T_K)$ behavior from the Kondo effect.

In summary, the large TEP of the host material makes the data analysis less straightforward than for noble-metal-based Kondo alloys. Using a provisional single-band picture we do see reasonably clear evidence for a Kondo effect but with T_K a factor of 10 or so larger than the earlier work. Band calculations of the TEP of PbTe as a function of hole doping might provide a further test of this conclusion.

We are grateful to T. H. Geballe, J. Schmalian, and V. Zlatić for their helpful comments. Work at Stanford was supported by the U.S. DOE, Office of Basic Energy Sciences under Contract No. DE-AC02-76SF00515 and that in Cambridge by the U.K. EPSRC-GB.

¹J. Kondo, *Prog. Theor. Phys.* **32**, 37 (1964).

²J. Kondo, in *Solid State Physics*, edited by F. Seitz, D. Turnbull, and H. Ehrenreich (Academic Press, New York, 1969), Vol. 23, p. 183.

³A. C. Hewson, *The Kondo Problem to Heavy Fermions* (Cambridge University Press, New York, 1993).

⁴M. Dzero and J. Schmalian, *Phys. Rev. Lett.* **94**, 157003 (2005).

⁵Y. Matsushita, H. Bluhm, T. H. Geballe, and I. R. Fisher, *Phys. Rev. Lett.* **94**, 157002 (2005).

⁶Y. Matsushita, P. A. Wianeci, A. T. Sommer, T. H. Geballe, and I. R. Fisher, *Phys. Rev. B* **74**, 134512 (2006).

⁷Y. Matsushita, Ph.D. thesis, Stanford University, 2007.

⁸Obtained from Lake Shore Cryotronics, Inc., Westerville, Ohio, U.S.A.

⁹I. A. Campbell, A. D. Caplin, and C. Rizzuto, *Phys. Rev. Lett.* **26**, 239 (1971).

¹⁰D. K. C. Macdonald, *Thermoelectricity: An Introduction to the Principles* (John Wiley and Sons, Inc., New York, 1962).

¹¹J. R. Cooper, L. Nonveiller, P. J. Ford, and J. A. Mydosh, *J. Magn. Magn. Mater.* **15-18**, 181 (1980).

¹²J. R. Cooper and P. J. Ford, *Philos. Mag. B* **65**, 1275 (1992).

¹³J. W. Loram, in *Morgins Conf.*, Solid State Physics, cited by A. J. Heeger, edited by F. Seitz, D. Turnbull, and H. Ehrenreich (Academic Press, N.Y., 1969), Vol. 23, p. 283.

¹⁴J. R. Cooper, Z. Vučić, and E. Babić, *J. Phys. F: Met. Phys.* **4**, 1489 (1974).

¹⁵C. Rizzuto, *Rep. Prog. Phys.* **37**, 147 (1974).

¹⁶J. M. Ziman, *Electrons and Phonons* (Clarendon Press, Oxford, U.K., 1960), Chap. 9.

¹⁷We also analyzed the TEP data for $x \geq 0.3\%$ using the original NG method, plotting S vs $1/\rho$ at fixed T . These NG plots deviated from linearity below 140 K. We believe this is mainly caused by small-angle scattering processes having a larger effect on thermal transport than on the electrical conductivity. Using two different extrapolation procedures to take this into account, we again found a positive peak in $S_K(T)$ near 50 K.

¹⁸J. R. Cooper and M. Miljak, *J. Phys. F: Metal Phys.* **6**, 2151 (1976).

¹⁹G. V. Lashkarev, R. O. Kikodze, and A. V. Brodovoi, *Sov. Phys. Semicond.* **12**, 633 (1978).